

Article

# Impact of Two Lavender Extracts on Silver Nanoparticle Synthesis, and the Study of Nanoparticles' Antibiofilm Properties and Their Ability to Transfer them into a Nontoxic Polymer

Lívia Mačák <sup>1,\*</sup>, Oksana Velgosova <sup>1</sup>  and Silvia Dolinská <sup>2</sup>

<sup>1</sup> Institute of Materials and Quality Engineering, Faculty of Materials Metallurgy and Recycling, Technical University of Košice, Letná 9/A, 042 00 Košice, Slovakia; oksana.velgosova@tuke.sk

<sup>2</sup> Institute of Geotechnics, Slovak Academy of Sciences, Watsonova 45, 040 01 Košice, Slovakia; sdolinska@saske.sk

\* Correspondence: livia.macak@tuke.sk; Tel.: +421-55-602-2776; Fax: +421-55-602-2770

**Abstract:** In this work, we aimed to analyze the impact of extracts prepared from dried *Lavandula angustifolia* (lavender) flowers and leaves on the synthesis of silver nanoparticles (AgNPs) (wherein the shape and size of AgNPs and the efficiency of the process were analyzed) and to prove the possibility of transferring the AgNPs' properties into a polymer matrix. An ex situ method was used to incorporate AgNPs and prepare polymer matrix composite (PVP-AgNPs) films (via casting) and fibers (via electrospinning). We used UV-vis absorption spectrophotometry, Fourier Transform Infrared Spectroscopy (FTIR), Transmission Electron Microscopy (TEM), and Scanning Electron Microscopy (SEM) to analyze and characterize the AgNPs and prepared composites. The results of FTIR analysis confirmed the presence of phytochemicals that can reduce silver ions from Ag<sup>+</sup> to Ag<sup>0</sup> in both extracts. The presence of spherical nanoparticles was confirmed via TEM regardless of the type of extract used. However, leaf extract caused the formation of AgNPs with a narrower size interval (an average size of 20 nm), and with higher efficiency, compared to the nanoparticles prepared using the flower extract. The nanoparticles prepared using the leaf extract were then incorporated into the polymer matrix, and thin polymer composite films and fibers were successfully prepared. The anti-biofilm activity of AgNPs colloids and prepared polymer nanocomposites against green algae *Chlorella kessleri* was studied. The anti-biofilm properties of the AgNPs were proved, along with the efficient transfer of their toxic properties into nontoxic polymer.

**Keywords:** AgNPs; green synthesis; lavender extracts; polymer nanocomposite; antibiofilm activity



**Citation:** Mačák, L.; Velgosova, O.; Dolinská, S. Impact of Two Lavender Extracts on Silver Nanoparticle Synthesis, and the Study of Nanoparticles' Antibiofilm Properties and Their Ability to Transfer them into a Nontoxic Polymer. *Micro* **2023**, *3*, 879–891. <https://doi.org/10.3390/micro3040060>

Received: 13 October 2023

Revised: 10 November 2023

Accepted: 15 November 2023

Published: 17 November 2023



**Copyright:** © 2023 by the authors. Licensee MDPI, Basel, Switzerland. This article is an open access article distributed under the terms and conditions of the Creative Commons Attribution (CC BY) license (<https://creativecommons.org/licenses/by/4.0/>).

## 1. Introduction

Nanoparticles are a modern material that is currently gaining a lot of attention and moving to the forefront not only in science but also in everyday life. These particles not only have unique properties that can enrich other materials, if used, for example, as a filler, but are also economically more advantageous compared to bulk materials. One of the key characteristics of nanoparticles is their size, which ranges from 1 to 100 nm [1]. This extremely small size range enables different properties compared to macroscopic materials. Properties such as melting point, reactivity, conductivity, and optical characteristics change with changing particle size [2], making nanoparticles suitable for application in many industries. Their antibacterial properties are used in medicine [3], the food industry [4], cosmetics [5], and the textile industry [6]. Conductive properties are often used in the electrical industry. Nanoparticles with catalytic properties [7] have wide applications in many fields, including energy, environmental engineering, and the chemical industry. In the energy sector, nanoparticles are used, for example, in the field of solar panels [8]. Their

surface properties and ability to catalyze [9] chemical reactions enable an increase in the efficiency of the conversion of solar energy into electrical energy. Nanoparticles can also be used in fuel cells, where they ensure faster and more efficient chemical reactions to produce electricity. In the field of environmental engineering, nanoparticles with catalytic properties can help clean wastewater and air. In the chemical industry, nanoparticles are used to accelerate chemical reactions and increase the yield of production processes [10,11]. Their small sizes and high surface area enable effective interaction with reactants and thus increase the speed and efficiency of reactions [12].

Nanoparticles can be produced using various methods, with the main methods being top-down (physical and physicochemical methods) and bottom-up (syntheses and reactions). The top-down methods include processes such as mill grinding, laser ablation, chemical vapor deposition (CVD), and others. These procedures focus on breaking down larger material structures into nanoparticles.

On the contrary, bottom-up methods (chemical and biological) are based on synthesis and reactions that enable the gradual construction of nanoparticles from molecular or atomic components [13]. Synthesis using chemical agents represents an environmental burden compared to synthesis that uses biomaterial [14]. In the biological (green) approach, natural resources and biologically active compounds present in plants are used to synthesize nanoparticles. However, biosynthesis also has its disadvantages, one of which is the possibility of inappropriately choosing a biomaterial, which can lead to overpricing and time extension of the entire nanoparticle production process. Therefore, it is necessary to choose a biomaterial whose properties, such as seasonal and geographical availability without time limitation, the ability to be easily handled, fast growth, and amenability to the simple preparation of an extract, are suitable for the effective synthesis of nanoparticles [15,16]. One of the most important factors when choosing a biomaterial is its composition. FTIR analysis makes it possible to determine the composition of a biomaterial. It enables the determination of functional groups such as phenols, flavonoids, peptides, proteins, and others found in biomaterials. The composition of plants is very complex, and therefore it is difficult to determine which components are responsible for stabilization and which are responsible for reduction. Based on the available research [17–19], in which biological materials were used in the synthesis of nanoparticles, it can be concluded that it is mainly proteins and flavonoids that are responsible for the reduction and stabilization of nanoparticles.

The use of biological synthesis for the preparation of AgNPs from plant sources opens new perspectives in the field of green and sustainable technologies [20,21]. Intensive studies centered around the production of various types of nanoparticles are currently underway. Although work on the preparation of AgNPs via green synthesis has been published many times, so far, no work has reported a comparison of the effect of using different parts of the same plant on synthesis.

The aim of this work was the biosynthesis and preparation of silver nanoparticles using lavender extracts, specifically to compare the effect of extracts from dry lavender leaves and flowers. This work also provides knowledge about the main components responsible for the reduction and stabilization of synthesized AgNPs, the influence of storage conditions on the stability of AgNP colloids, and the toxic/antibiofilm properties of AgNPs. The other contributions of this work are the incorporation of prepared AgNPs into a polymer matrix composite (PMC) and the fabrication of polymer-based non-woven fabrics (electrospinning) and thin layers (casting) whose properties are enriched by the addition of AgNPs. For PMC preparation, an *ex situ* method was used, and polyvinyl alcohol (PVA) and prepared AgNPs were used as a matrix and a secondary phase, respectively.

## 2. Materials and Methods

### 2.1. Materials

Lavender flowers and leaves were collected in a local garden in Košice (Slovakia) during the flowering period (July). As a precursor, silver nitrate ( $\text{AgNO}_3$ ) (99.8%) was

used, which was purchased from Penta Chemical Unlimited. Deionized water was used for solution preparation, dilution, and washing. Polyvinyl alcohol (PVA) (M.W. of approx. 146,000–186,000, purchased from Mikrochem Ltd., Pezinok, Slovakia) was used as a matrix to produce a polymer matrix composite doped with AgNPs.

### 2.2. Preparation of Flower and Leaf Extracts

Two types of extracts were prepared for the experiment. Lavender flowers and leaves were collected, washed twice with deionized water, and dried at 45 °C. Both dried flowers and leaves were crushed in a mortar and then mixed with 100 mL of deionized water. In a water bath, the mixtures were heated to a temperature ranging from 70 to 80 °C for 10 min. Such a temperature range was chosen to achieve good transfer of natural substances (contained in plant cells) to the extract.

Subsequently, the mixtures were allowed to cool, and the solid component was separated using filter paper. The filtered solutions were centrifuged at 9000 rpm for 30 min. The prepared extracts were kept in a refrigerator for further experiments. Figure 1 shows the AgNO<sub>3</sub> stock solution and extracts prepared from the dried lavender flower (Ex-F) and leaves (Ex-L).

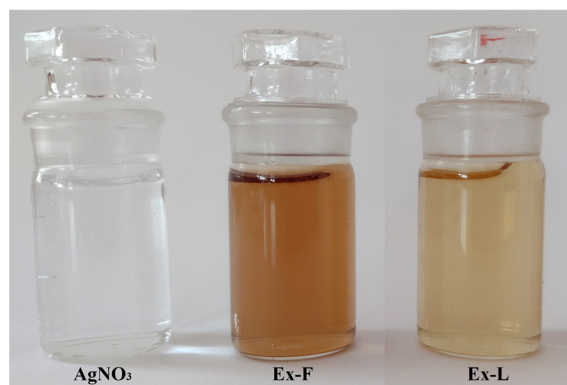


**Figure 1.** AgNO<sub>3</sub> solution and extracts of dried lavender flowers (Ex-F) and leaves (Ex-L).

### 2.3. Preparation of AgNPs

Two Erlenmeyer flasks were prepared, and 100 mL of AgNO<sub>3</sub> stock solution with a concentration of  $c = 50$  mg/L was poured into each of them. Both AgNO<sub>3</sub> solutions were placed on stirrers with heating applied and stirred until the temperature of the solutions reached 80 °C. Subsequently, 20 mL of dry flower extract was added to the first solution (labeled AgNPs-F), and 20 mL dry leaf extract (labeled AgNPs-L) was added to the second. After adding the extracts into the AgNO<sub>3</sub>, it was possible to observe a change in coloration from light brown to dark brown transpiring within a few minutes. This color change implied the formation of AgNPs. Subsequently, after cooling, the solutions were subjected to UV-vis analysis and stored under different conditions to monitor stability.

### 2.4. Stability of AgNPs Solutions

Prepared nanoparticle solutions (120 mL each) were divided into four 60 mL Erlenmeyer flasks. The stability of nanoparticles under two conditions was monitored, and the solutions were labeled as follows:

- F-Cold—colloidal nanoparticles prepared using Ex-F, stored in a refrigerator (5 °C) in the dark.
- L-Cold—colloidal nanoparticles prepared using Ex-L, stored in a refrigerator (5 °C) in the dark.
- F-RT—colloidal nanoparticles prepared using Ex-F, stored at room temperature (25 °C) under light/dark conditions for 12:12 h.

- L-RT—colloidal nanoparticles prepared using Ex-L, stored at room temperature (25 °C) under light/dark conditions for 12:12 h.

### 2.5. Preparation of PMC

The ex situ method was used to prepare the PVA-AgNPs nanocomposite. PVA is a water-soluble synthetic polymer. It is colorless, odorless, biocompatible, and non-toxic. PVA is used for a variety of applications, such as vascular stents, cartilage, contact lenses, etc.

PVA polymer was used as a matrix, and AgNPs (prepared via biological synthesis using Ex-L) were used as a secondary phase. To prepare 50 mL of PVA-AgNPs solution (8%), PVA powder and freshly prepared colloidal AgNPs were mixed at 80 °C for 1 h to achieve a uniform distribution of AgNPs. The PVA-AgNP composite solution was used to create nonwoven textiles (fibers) using the electrospinning technique and thin films via room-temperature casting. The voltage used in the electrospinning process was 82 kV, and the distance between the rotating and receiving electrodes was 150 mm.

### 2.6. Characterization of Extracts, AgNP Colloids, and PMC Doped with AgNPs

The compositions of the extracts were analyzed using an FTIR spectrometer. The infrared spectra were recorded using a Bruker Tensor 27 FTIR spectrometer equipped with DTGS KBr detector. For each sample, 64 scans were conducted in the 4000–400  $\text{cm}^{-1}$  spectral range in abs mode with a resolution of 4  $\text{cm}^{-1}$ . The KBr pressed-disc technique was used to prepare a solid sample for routine scanning of the spectra. Samples of approximately 0.1 mg were dispersed in 150 mg of KBr to record optimal spectra in the 4000–400  $\text{cm}^{-1}$  region. The diameter of the pellets, pressed from samples, was 13 mm.

Prepared AgNP colloidal solutions were analyzed using a UV-vis spectrophotometer (UNICAM UV-vis Spectrophotometer UV4). Samples were measured on days 1, 3, 7, 10, 14, and 21 in the wavelength range of 350–700 nm; as a control, a mixture of H<sub>2</sub>O/extract in a ratio of 5:1 was used. UV-Vis spectrophotometry is used to measure light absorption in the ultraviolet and visible spectra. By analyzing the UV-vis spectra results, it is possible to predict the shapes of nanoparticles and their relative concentrations and approximate sizes. In the case of a change in the shape of the spectra with time, it is possible to predict a change in shape, size, or agglomeration of nanoparticles.

The size and morphology of the nanoparticles were studied using TEM (JEOL model JEM-2000FX, with an accelerating voltage of 200 kV) and SEM/FIB (SEM/FIB ZEISS-AURIGA Compact). Thanks to the results of both imaging techniques, we obtained a more comprehensive view (nano-level) of the samples. The findings from TEM and SEM analysis complement each other and provide more complex data about the sample. In TEM analysis, electrons pass through a sample. Thus, a 2D image can be obtained, from which the shapes and sizes of the nanoparticles can be determined. SEM analysis is based on scanning the surface of a sample, and the output is a 3D image. This 3D image provides real information about the morphology of the sample. It is also possible to determine the size of the particles, and with the help of EDX analysis, we can determine the elemental composition of a sample [22]. The image analysis (ImageJ software 1.53e) was used for the analysis of the Ag nanoparticles' size distribution; at least 300 nanoparticles for each sample were measured to determine the size distribution.

### 2.7. Antibiofilm Activity

The antibiofilm activity of AgNPs was evaluated using the standard disk-diffusion method described by Kavita et al. with some modifications [23]. Milieu Bristol agar plates in Petri dishes were inoculated with green algae *Chlorella kessleri* in a sterile box. The 15  $\mu\text{L}$  of prepared extracts (Ex-F and Ex-L) and the AgNP colloidal solutions (AgNPs F and AgNPs L) were plated on agar plates using sterile swabs. Afterwards, the agar plates were incubated at room temperature under dark/light conditions for 12:12 h. Three replicate samples were tested for each condition. Control tests with AgNO<sub>3</sub> were also conducted.

The presence and size of the inhibition zone on the agar plates were checked after 14 days of growth.

Samples of PVA-AgNPs composite fibers and thin layers were cut out in the form of discs and directly placed on an agar plate that was inoculated with the green algae *Chlorella kessleri*. Antibiofilm activity of polymer composites was observed under the same conditions applied for the previous samples.

### 3. Results

#### 3.1. FTIR Analysis

FTIR analysis is a method used to determine the functional groups of an organic or inorganic sample. The principle here is that the different functional groups absorb IR radiation with a frequency that is characteristic of the given context [24]. Lavandula is known for its medicinal properties and contains various compounds that can serve as reducing agents and stabilizers in the process of AgNP formation. Figure 2 shows the FTIR spectra of the extracts prepared from the dried lavender flowers (Ex-F) and leaves (Ex-L).

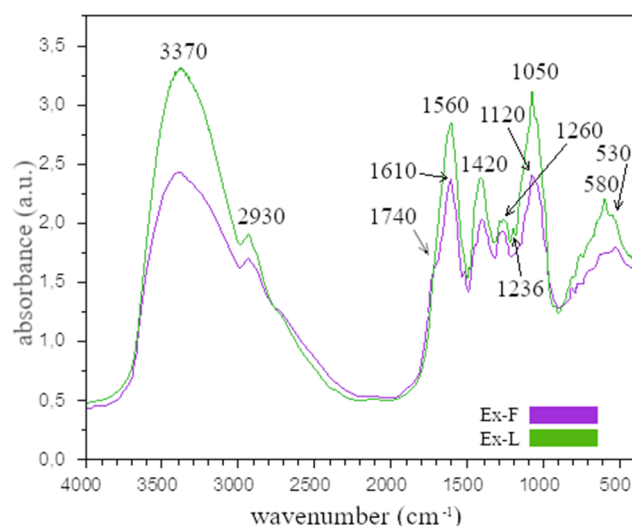


**Figure 2.** IR spectra of extracts prepared from dried lavender flowers (Ex-F) and leaves (Ex-L).

From the comparison of the FTIR analysis of Ex-F and Ex-L, it is clear that the absorption bands are similar for both cases. The wide band around the value of  $3370\text{ cm}^{-1}$  (O–H) confirms the presence of alcohol. The absorption bands in the range of  $2800\text{--}3000\text{ cm}^{-1}$  are valence and deformation vibrations of C–H bonds in methyl and methylene disorders. The band at  $1740\text{ cm}^{-1}$ , which was only observed for Ex-F, corresponds to the valence vibration of the C=O group. This band was also confirmed by other authors [25–27] and may be due to the presence of the carbonyl groups of the esters, which may be associated with a double bond or an aromatic ring [28]. The absorption band at  $1610\text{ cm}^{-1}$  is associated with the valence vibrations of C=C groups [29,30], while the absorption band at around  $1560\text{ cm}^{-1}$  may be due to the presence of amide I and amide II, which arise from carbonyl and -N–H valence vibrations in the amide bonds of proteins. The band at  $1420\text{ cm}^{-1}$  corresponds to the C–O–H group. The absorption bands at the wavelength of  $1380\text{ cm}^{-1}$  correspond to C–H vibrations and, as in the case of the bands in the range of  $2800\text{--}3000\text{ cm}^{-1}$ , were caused by valence and deformational vibrations of C–H bonds in methyl and methylene groups [30]. The absorption band at the wavelength around  $1236\text{ cm}^{-1}$  and the band around  $1120\text{ cm}^{-1}$  can be assigned to the C–O valence vibration of the ester group [26,27]. The absorption band that appeared in the spectra at the wavelength of around  $1050\text{ cm}^{-1}$  is related to the C–O bond. The bands at  $580$  and  $530\text{ cm}^{-1}$  were caused by alkyl halides, which are found in flavonoids.

The similarity of the spectra of both extracts is understandable since they originate from the same plant. The composition of lavender is very complex; e.g., Umezu et al.

analyzed the essential oil of the lavender flower, identifying 26 components, among which were  $\alpha$ -pinene, camphene,  $\beta$ -myrcene, p-cymene, limonene, cineol linalool, and camphor tannins [29]. Further, more detailed research and analysis of lavender flower proved the presence of more than a few other components, and this presence depended on the place of cultivation and the time of harvest. Most authors agree that the main components of lavender flower oil are linalool and linalyl acetate [27,31]. Above all, these two main components have anti-inflammatory, antifungal, and antibacterial properties [27]. As in the case of the flower, lavender leaf also contains many components; among the leaf's essential oils are eucalyptol, camphor, and borneol [30].

The FTIR spectra of the colloidal solutions prepared using both extracts, shown in Figure 3a,b, were like the spectra of the individual extracts, indicating the presence of some phytochemicals from the plant extract. It is obvious that the bands in the FTIR spectra presented the greatest degree of similarity.

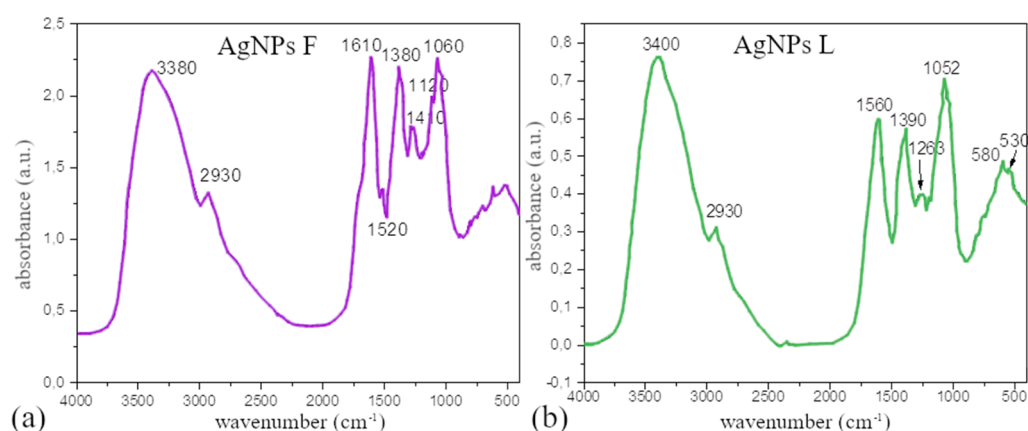


**Figure 3.** FTIR spectra of AgNPs colloids prepared using (a) Ex-F and (b) Ex-L.

However, after the reduction of  $\text{Ag}^+$  ions to  $\text{Ag}^0$ , there is a noticeable difference in the intensity or shift of some of the bands. We assume that the phytochemicals that experienced the changes are responsible for the reduction and/or stabilization of the AgNPs. A change in bands after synthesis was also observed by other authors [32], and based on our results and the conclusions of other authors, it is possible to select the components responsible for the reduction and stabilization of AgNPs. According to the authors of [32], the decrease in bands belonging to phenolic flavonoids, free groups present in proteins and flavonoids, could be responsible for the reduction of silver ions to silver nanoparticles and coating the nanoparticles to stabilize them and to prevent their aggregation. It is very difficult to accurately separate the components responsible for reduction from those responsible for stabilization. Most authors agree that plant extract components such as carbonyl groups from esters or essential oils, which are the main components of these leaves, could form a layer around metal nanoparticles that could contribute to the stabilization of the nanoparticles [33,34].

### 3.2. UV-Vis Analysis

UV-vis analysis is a simple method used to verify the presence of nanoparticles in solutions. For spherical AgNPs, it is characteristic for the maximum of the Surface Plasmon Resonance (SPR) band to be within the wavelength interval of 350–450 nm [26,29]. Based on the shape, location, and size of the peak, the size, size distribution, and shape of the nanoparticles can be approximately determined. Figure 4 shows the SPR bands of nanoparticles prepared using leaf and flower extracts measured immediately after synthesis. The figure shows that regardless of the extract used,  $ABS_{max}$  was measured at a wavelength of 424 nm, which confirms the presence of AgNPs [35–39]. In both cases, a reducing ability of the extracts was confirmed. At the same time, it is clear that there are more nanoparticles in the colloidal silver solution prepared using Ex-L because  $ABS_{max}$  has a higher value than it does in the colloidal solution prepared using Ex-F. Based on the SPR band shape and the

colloidal solution AgNP L, which is slimmer and more symmetrical compared to the AgNP F solution, it is obvious that the nanoparticles in the AgNP L solution are in a narrower size interval. The same conclusions from the SPR band for AgNPs prepared using green synthesis were drawn by Kumar et al. [30].

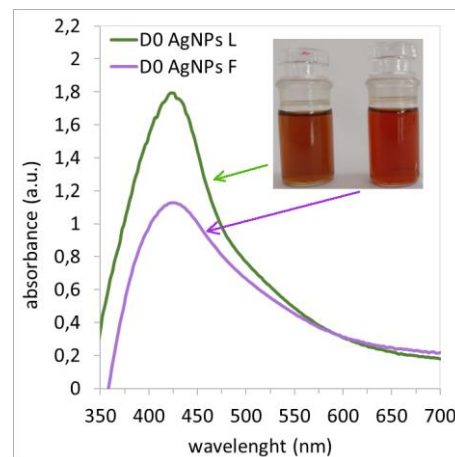


**Figure 4.** UV-vis absorption spectra of synthesized AgNPs (day 0) prepared using lavender flower (D0 AgNPs F) and leaf (D0 AgNPs L) extracts.

Another important property is the stability of nanoparticles, which depends on several factors, such as the presence of stabilizing substances in the extracts and storage conditions (RT, cold temperatures, etc.). The stability of the AgNPs in colloidal solution for the samples stored at room temperature and in a refrigerator (F-RT, F-Cold, L-RT, and L-Cold) was monitored over 21 days (Figure 5).

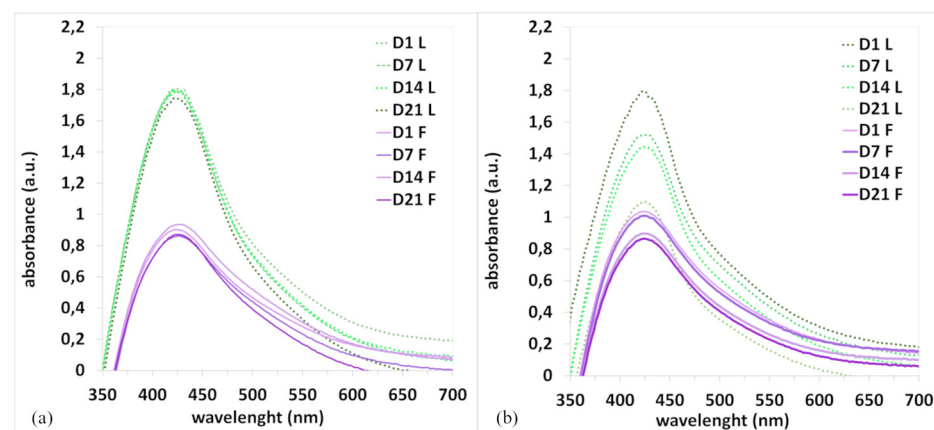


**Figure 5.** UV-vis spectra of AgNPs F and AgNPs L stored in the cold (a) and at room temperature (b).

From the course of the SPR bands (Figure 5a), it is clear that the colloids of the nanoparticles prepared using Ex-L and Ex-F stored in the cold were stable during the entire experiment because no changes in the shape or position of the bands can be observed. Figure 5b provides a comparison of the colloidal solutions stored at room temperature. The graph shows that storage conditions adversely affect stability. Degradation of nanoparticles occurred, and a significant decrease in SPR bands and a shift in  $ABS_{max}$  were observed in both cases (Figure 5b). It is clear that the stability of colloids strongly depends on the storage conditions. The experiments confirmed that the combination of a low temperature and dark conditions is the best choice for securing nanoparticle stability.

For all the colloidal solutions stored in a refrigerator and at room temperature, the pH was measured over 21 days (Figure 6). The colloidal solutions stored at room temperature

have larger deviations, and, in general, their pH values increased. In the case of the colloids stored in the cold, the pH did not change significantly, which means that the extracts, due to their composition, provide a suitable and stable environment. Silver nanoparticles are well known for being sensitive to light. We assume that this factor causes their degradation, which is reflected in the increase in pH values.

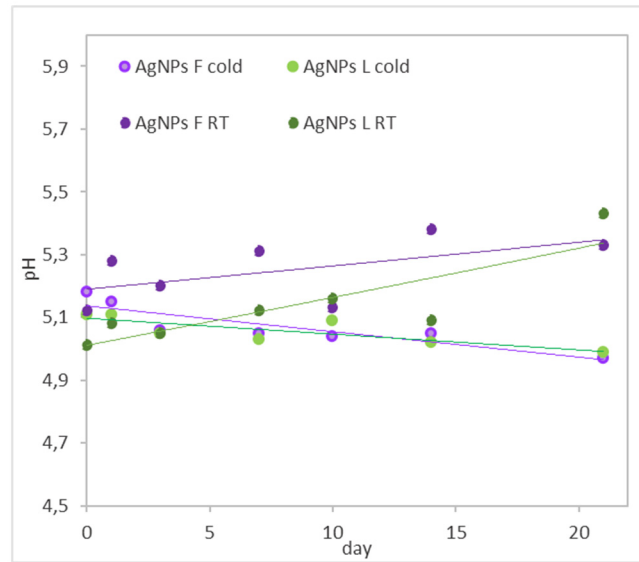


**Figure 6.** The pH of AgNP colloids prepared using Ex-F and Ex-L.

### 3.3. TEM and SEM Analysis

Using TEM analysis, the morphology and sizes of the AgNPs were determined. Figure 7a,c show TEM microphotographs of AgNPs prepared using Ex-F and Ex-L (day 0) and their size distribution. The results of the TEM analysis confirmed the presence of nearly spherical nanoparticles in both cases. However, in the case of Ex-L, the presence of smaller nanoparticles was observed, 75% of which were up to an average size of 20 nm. In the case of Ex-F, only 60% were up to 20 nm in size, and a small number of ~50 nm nanoparticles were also observed.

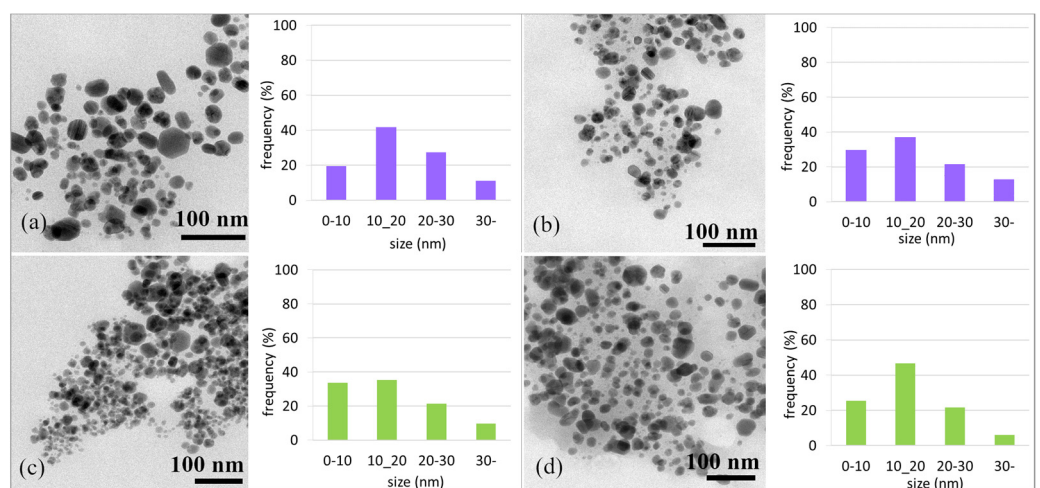


**Figure 7.** TEM micrograph of AgNPs F and size distribution of nanoparticles at D0 (a); TEM micrograph of AgNPs F and size distribution of nanoparticles on D21 (b); TEM micrograph of AgNPs L and size distribution of nanoparticles at D0 (c); TEM micrograph of AgNPs L and size distribution of nanoparticles on D21 (d).

Figure 7b,d show the TEM microphotographs of the AgNPs stored in cold conditions, i.e., in a refrigerator. After 21 days, the shapes of the nanoparticles did not change. A slight change in the number of nanoparticles with a size of up to 20 nm (from 75% to 80% in the case of Ex-L and from 60% to 69% for Ex-F) was observed; such changes are not significant. The difference in the size distribution results could be due to statistical variation in the measurement of the distribution.

Analysis via scanning electron microscopy confirmed the presence of uniform, almost-spherical AgNPs, as shown in Figure 8a,b. EDX analysis, the results of which are shown in Figure 8a,b, confirmed the presence of silver and demonstrated the presence of signals of accompanying elements such as C, Cl, O, and Ca. These elements probably came from the biological component of the extract, which could be removed by washing the samples more thoroughly with ethanol.

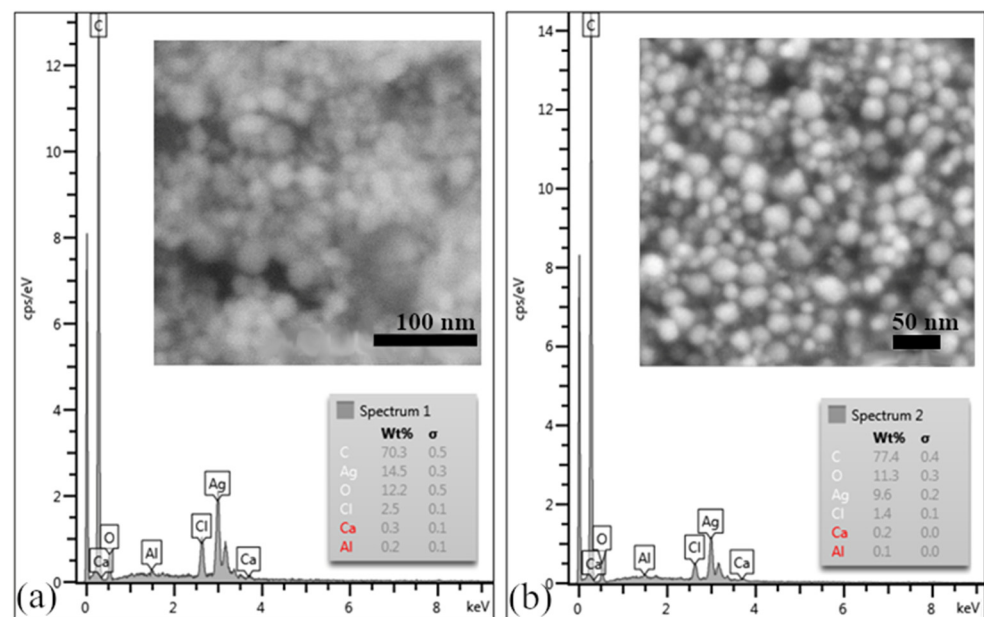


**Figure 8.** (a) EDX analysis of sample AgNPs F; the inner picture shows SEM microstructure of AgNPs prepared using Ex-F. (b) EDX analysis of sample AgNPs L; the inner picture shows SEM microstructure of AgNPs prepared using Ex-L.

### 3.4. Polymer Matrix Nanocomposite

Polyvinyl alcohol (PVA) is a polymer used in various industrial applications to produce plastics and plastic products such as packaging materials. It is also used to produce textile fibers as well as material used in the field of medicine. In addition, PVA is a biodegradable polymer, which means that it can break down in the environment and does not have an impact on the environment.

For the preparation of polymer composites, PVA was used as a matrix, and AgNPs prepared using Ex-L were used as a secondary phase. Composite PVA-AgNPs thin layers and fibers were prepared. The structures of the prepared PMC layers, shown in Figure 9a, and fibers, shown in Figure 9b, were observed using SEM. In both cases, it is obvious that the nanoparticles are not evenly distributed.

Nanoparticles in thin films are unevenly distributed and form clusters; the detailed view of the cluster (inner picture) confirms this. An uneven distribution can also be observed in the fibers (Figure 9b). Nanoparticles in fibers were distributed individually, in clusters, or in chains (induced using the electrospinning technique). They can be observed on the surfaces of the fibers, as shown in Figure 9c, and inside them, as shown in Figure 9d.

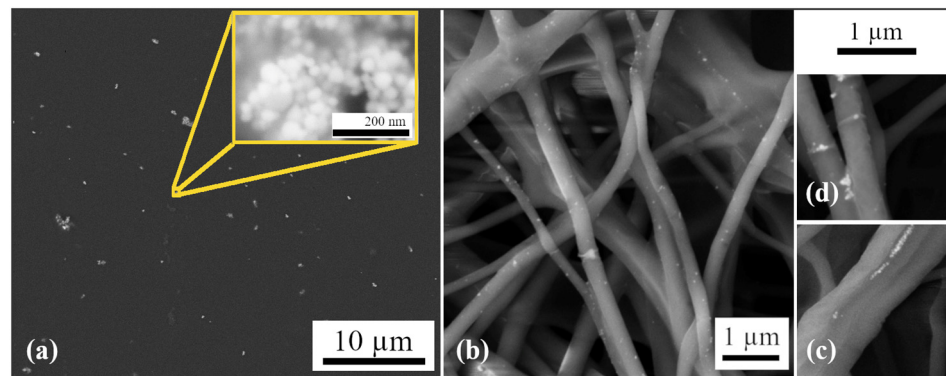


**Figure 9.** (a) SEM image of a thin film with AgNPs L; the inner picture shows SEM microstructures of AgNPs prepared using Ex-L. (b) SEM image of fibers with AgNPs L. (c) Details of AgNPs in fibers. (d) Details of AgNPs on fibers.

Despite homogenization via ultrasound and the use of mixing, it was not possible to ensure a homogeneous distribution of nanoparticles. The uneven distribution of nanoparticles in the polymer solution might have been caused by the high density of the polymer solution. The key to increasing the homogeneity could be the preparation of a PVA solution with lower density and better homogenization (sonification and intense mixing under heat).

### 3.5. Antibiofilm Activity

Much research has aimed to demonstrate the biocidal effects of silver on various types of viruses, bacteria, fungi, and algae, but few studies have aimed to elucidate the mechanisms by which silver develops toxicity. The available sources show that the most likely mechanisms behind the toxicity of AgNPs or released  $\text{Ag}^+$  ions include disruption of the functionality of the cell wall and cell membranes, reactive oxygen species (ROS) formation, and DNA replication disorders [40,41].

The antibacterial activity of AgNPs was investigated in comparison to the alga *Chlorella kessleri* using a modified disc diffusion method. *Ch. kessleri* is a unicellular, freshwater, green, non-toxic, environmentally safe, and easy to cultivate alga.

Antibiofilm activity was monitored for 14 days. Lavender flower and leaf extracts were applied, and  $\text{AgNO}_3$  stock solution was used as a control. The extracts themselves, shown in Figure 10b,d, and  $\text{AgNO}_3$  did not show any inhibition zones during the 14 days of observation.

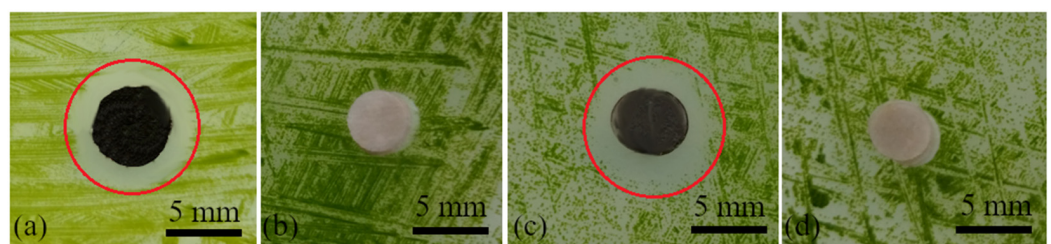


**Figure 10.** (a) Antibiofilm activity of AgNPs F, (b) antibiofilm activity of Ex-F, (c) antibiofilm activity of AgNPs L, and (d) antibiofilm activity of Ex-L.

However, the colloidal nanoparticles prepared using different extracts dropped onto the discs, shown in Figure 10a,c, showed significant inhibition zones of 9.0 mm and 9.3 mm for AgNPs-F and AgNPs-L, respectively.

Antibiofilm activity was also monitored for the produced PMCs. Samples of the AgNP-containing polymer solution (Figure 11a), fibers (Figure 11b), and the thin film (Figure 11c) were placed on inoculated agar.

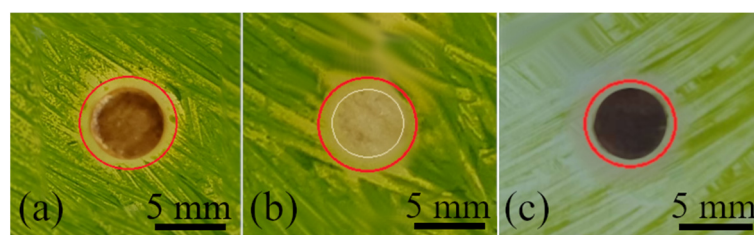


**Figure 11.** (a) Antibiofilm activity of PVA-AgNPs L solution, (b) antibiofilm activity of AgNPs L fibers, and (c) antibiofilm activity of AgNPs L film.

The inhibition zones formed after 14 days were not as significant as those in the case of the colloidal solutions but were visible and ranged from 7 mm to 8 mm in diameter. The formation of narrower inhibition zones could be due to the poor distribution of AgNPs in the PMC, as shown via SEM analysis, and the fact that the nanoparticles were coated/surrounded by the polymer (only a small percentage of the nanoparticles were on the surface). Therefore, there was no immediate contact of the AgNPs with living cells; only a gradual release of the nanoparticles occurred. This, on the other hand, can be considered an advantage because gradual release contributes to prolonging the antibacterial effect.

#### 4. Conclusions

In this study, silver nanoparticles were successfully synthesized via a biological method using two different lavender extracts (flowers and leaves). Storage conditions were also determined, and these conditions will ensure the long-term stability of the prepared colloids. The ability of AgNPs to prevent the formation of biofilms was also confirmed, and the synthesized nanoparticles were successfully incorporated into the polymer matrix (PVA-AgNPs), which caused the change in the PVA's nature from non-toxic to toxic.

Using both extracts, nearly spherical and uniform nanoparticles with a size of around 20 nm were synthesized. However, the extract prepared from the leaves achieved higher yields, and the AgNPs were in a narrow size interval. Long-term stability tests were carried out under different conditions; it was shown that cold storage can ensure good stability of nanoparticles regardless of extract type and storage time. During the toxicity test, the prepared AgNP colloids created significant inhibition zones, proving their antibiofilm effect.

The *ex situ* method was used for the preparation of PVA-AgNPs composites. Thin layers were subsequently prepared using casting and fibers via electrostatic spinning. SEM analysis showed that AgNPs formed clusters in the polymer matrix, indicating the need to improve the distribution of AgNPs in the matrix. However, despite the uneven distribution, it was proven that AgNPs successfully transferred antibacterial properties to the originally non-toxic PVA, indicating the possibility of transferring other properties, e.g., catalytic, conductive, etc. However, these properties significantly depend on the shape and volume of the incorporated nanoparticles.

The results provide a sustainable and ecological method for the synthesis of AgNPs and highlight the potential of biological extracts in the synthesis and stabilization of nanoparticles. These findings have important implications for the fields of nanotechnology and the development of antibacterial materials, suggesting practical applications in various industries.

**Author Contributions:** Conceptualization, L.M. and O.V.; methodology, L.M., O.V., and S.D.; validation, L.M. and O.V.; formal analysis, L.M., O.V., and S.D.; writing—original draft preparation, L.M.; writing—review and editing, L.M. and O.V.; visualization, O.V. All authors have read and agreed to the published version of the manuscript.

**Funding:** This research received no external funding.

**Data Availability Statement:** Data are contained within the article.

**Acknowledgments:** This work was financially supported by the Slovak Grant Agency (VEGA 1/00220/22).

**Conflicts of Interest:** The authors declare no conflict of interest.

## References

1. Khan, I.; Saeed, K.; Khan, I. Nanoparticles: Properties, applications and toxicities. *Arab. J. Chem.* **2019**, *12*, 908–931. [[CrossRef](#)]
2. Altammar, K.A. A review on nanoparticles: Characteristics, synthesis, applications, and challenges. *Front. Microbiol.* **2023**, *14*, 1155622. [[CrossRef](#)]
3. Xu, L.; Wang, Y.Y.; Huang, J.; Chen, C.Y.; Wang, Z.X.; Xie, H. Silver nanoparticles: Synthesis, medical applications and biosafety. *Theranostics* **2020**, *10*, 8996–9031. [[CrossRef](#)] [[PubMed](#)]
4. Carbone, M.; Donia, D.T.; Sabbatella, G.; Antiochia, R. Silver nanoparticles in polymeric matrices for fresh food packaging. *J. King Saud Univ.—Sci.* **2016**, *28*, 273–279. [[CrossRef](#)]
5. Yadwade, R.; Gharpure, S.; Ankamwar, B. Nanotechnology in cosmetics pros and cons. *Nano Express* **2021**, *2*, 022003. [[CrossRef](#)]
6. Gong, D.; Celi, N.; Zhang, D.; Cai, J. Magnetic Biohybrid Microrobot Multimers Based on *Chlorella* Cells for Enhanced Targeted Drug Delivery. *ACS Appl. Mater. Interfaces* **2022**, *14*, 6320–6330. [[CrossRef](#)] [[PubMed](#)]
7. Ibrahim, N.; Ahmad Zubir, S.; Abd Manaf, A.; Mustapha, M. Stability and conductivity of water-based colloidal silver nanoparticles conductive inks for sustainable printed electronics. *J. Taiwan Inst. Chem. Eng.* **2023**, *153*, 105202. [[CrossRef](#)]
8. Ounkaew, A.; Kasemsiri, P.; Srichiangsa, N.; Hiziroglu, S.; Maraphum, K.; Posom, J.; Chindaprasirt, P. Green synthesis of nanosilver coating on paper for ripening delay of fruits under visible light. *J. Environ. Chem. Eng.* **2021**, *9*, 105094. [[CrossRef](#)]
9. Parida, D.; Moreau, E.; Nazir, R.; Salmeia, K.A.; Frison, R.; Zhao, R.; Gaan, S. Smart hydrogel-microsphere embedded silver nanoparticle catalyst with high activity and selectivity for the reduction of 4-nitrophenol and azo dyes. *J. Hazard. Mater.* **2021**, *416*, 126237. [[CrossRef](#)] [[PubMed](#)]
10. Salata, O.V. Applications of nanoparticles in biology and medicine. *J. Nanobiotechnol.* **2004**, *2*, 3. [[CrossRef](#)]
11. Martínez, G.; Merinero, M.; Pérez-Aranda, M.; Pérez-Soriano, E.; Ortiz, T.; Villamor, E.; Alcudia, A. Environmental Impact of Nanoparticles' Application as an Emerging Technology: A Review. *Materials* **2020**, *14*, 166. [[CrossRef](#)]
12. Chaturvedi, S.; Dave, P.N.; Shah, N.K. Applications of nano-catalyst in new era. *J. Saudi Chem. Soc.* **2012**, *16*, 307–325. [[CrossRef](#)]
13. Choi, W.K.; Liew, T.H.; Chew, H.G.; Zheng, F.; Thompson, C.V.; Wang, Y.; Yun, J.A. Combined Top-Down and Bottom-Up Approach for Precise Placement of Metal Nanoparticles on Silicon. *Small* **2008**, *4*, 330–333. [[CrossRef](#)]
14. Liaqat, N.; Jahan, N.; Rahman, K.; Anwar, T.; Qureshi, H. Green synthesized silver nanoparticles: Optimization, characterization, antimicrobial activity, and cytotoxicity study by hemolysis assay. *Front Chem.* **2022**, *10*, 952006. [[CrossRef](#)] [[PubMed](#)]
15. Ying, S.; Guan, Z.; Polycarp, C.; Ofoegbu, B.; Clubb, P.; Rico, C.; He, F.; Hong, J. Green synthesis of nanoparticles: Current developments and limitations. *Environ. Technol. Innov.* **2022**, *26*, 102336. [[CrossRef](#)]
16. Nasiri, J.; Rahimi, M.; Hamezadeh, Z.; Motamedi, E.; Naghavi, M.R. Fulfillment of green chemistry for synthesis of silver nanoparticles using root and leaf extracts of *Ferula persica*: Solid-state route vs. solution-phase method. *J. Clean. Prod.* **2018**, *192*, 514–530. [[CrossRef](#)]
17. Priya, R.S.; Geetha, D.; Ramesh, P.S. Antioxidant activity of chemically synthesized AgNPs and biosynthesized *Pongamia pinnata* leaf extract mediated AgNPs—A comparative study. *Ecotoxicol. Environ. Saf.* **2016**, *134*, 308–318. [[CrossRef](#)] [[PubMed](#)]
18. Ballottin, D.; Fulaz, S.; Souza, M.L.; Corio, P.; Rodrigues, A.G.; Souza, A.O.; Tasic, L. Elucidating Protein Involvement in the Stabilization of the Biogenic Silver Nanoparticles. *Nanoscale Res. Lett.* **2016**, *11*, 313. [[CrossRef](#)]
19. Ullah, A.; Munir, S.; Badshah, S.L.; Khan, N.; Ghani, L.; Poulson, B.G.; Jaremko, M. Important Flavonoids and Their Role as a Therapeutic Agent. *Molecules* **2020**, *25*, 5243. [[CrossRef](#)]
20. Al Sufyani, N.M.; Hussien, N.A.; Hawsawi, Y.M. Characterization and Anticancer Potential of Silver Nanoparticles Biosynthesized from *Olea chrysophylla* and *Lavandula dentata* Leaf Extracts on HCT116 Colon Cancer Cells. *J. Nanomater.* **2019**, *2019*, 7361695. [[CrossRef](#)]
21. Bihal, R.; Al-Khayri, J.M.; Banu, A.N.; Kudesia, N.; Ahmed, F.K.; Sarkar, R.; Arora, A.; Abd-Elsalam, K.A. Entomopathogenic Fungi: An Eco-Friendly Synthesis of Sustainable Nanoparticles and Their Nanopesticide Properties. *Microorganisms* **2023**, *11*, 1617. [[CrossRef](#)]
22. Brodusch, N.; Brahimi, S.V.; Barbosa De Melo, E.; Song, J.; Yue, S.; Piché, N.; Gauvin, R. Scanning Electron Microscopy versus Transmission Electron Microscopy for Material Characterization: A Comparative Study on High-Strength Steels. *Scanning* **2021**, *2021*, 5511618. [[CrossRef](#)] [[PubMed](#)]
23. Kavita, K.; Singh, V.K.; Jha, B. 24-Branched  $\Delta^5$  sterols from *Laurencia papillosa* red seaweed with antibacterial activity against human pathogenic bacteria. *Microbiol. Res.* **2014**, *169*, 301–306. [[CrossRef](#)] [[PubMed](#)]
24. Kemp, W. *Organic Spectroscopy*; Macmillan Education: London, UK, 1991. [[CrossRef](#)]
25. Limban, C.; Marutescu, L.; Chifiriuc, M.C. Synthesis, Spectroscopic Properties and Antipathogenic Activity of New Thiourea Derivatives. *Molecules* **2011**, *16*, 7593–7607. [[CrossRef](#)] [[PubMed](#)]
26. Baláž, M.; Bedlovičová, Z.; Daneu, N.; Siksa, P.; Sokoli, L.; Tkáčiková, L.; Bujňáková, Z.L. Mechanochemistry as an Alternative Method of Green Synthesis of Silver Nanoparticles with Antibacterial Activity: A Comparative Study. *Nanomaterials* **2021**, *11*, 1139. [[CrossRef](#)] [[PubMed](#)]

27. Hajhashemi, V.; Ghannadi, A.; Sharif, B. Anti-inflammatory and analgesic properties of the leaf extracts and essential oil of *Lavandula angustifolia* Mill. *J. Ethnopharmacol.* **2003**, *89*, 67–71. [[CrossRef](#)]
28. Lafhal, S.; Vanloot, P.; Bombarda, I.; Kister, J.; Dupuy, N. Identification of metabolomic markers of lavender and lavandin essential oils using mid-infrared spectroscopy. *Vib. Spectrosc.* **2016**, *85*, 79–90. [[CrossRef](#)]
29. Kumar, B.; Smita, K.; Cumbal, L. Biosynthesis of silver nanoparticles using lavender leaf and their applications for catalytic, sensing, and antioxidant activities. *Nanotechnol. Rev.* **2016**, *5*, 521–528. [[CrossRef](#)]
30. Kumar, B.K.; Smita, K.S.; Vizuite, K.; Cumbal, L. Aqueous phase lavender leaf mediated green synthesis of gold nanoparticles and evaluation of its antioxidant activity. *Biol. Med.* **2006**, *8*, 3. [[CrossRef](#)]
31. Lugani, Y.; Sooch, B.S.; Singh, P.; Kumar, S. Nanobiotechnology applications in food sector and future innovations. In *Microbial Biotechnology in Food and Health*; Academic Press: Cambridge, MA, USA, 2021; pp. 197–225. [[CrossRef](#)]
32. Lafhal, S.; Vanloot, P.; Bombarda, I.; Kister, J.; Dupuy, N. Chemometric analysis of French lavender and lavandin essential oils by near infrared spectroscopy. *Ind. Crops Prod.* **2016**, *80*, 156–164. [[CrossRef](#)]
33. Elemike, E.E.; Onwudiwe, D.C.; Ekennia, A.C.; Katata-Seru, L. Biosynthesis, characterization, and antimicrobial effect of silver nanoparticles obtained using *Lavandula* × intermedia. *Res. Chem. Intermed.* **2016**, *43*, 1383–1394. [[CrossRef](#)]
34. Al-Otibi, F.; Al-Ahaidib, R.A.; Alharbi, R.I.; Al-Otaibi, R.M.; Albasher, G. Antimicrobial Potential of Biosynthesized Silver Nanoparticles by *Aaronsohnia factorovskyi* Extract. *Molecules* **2020**, *26*, 130. [[CrossRef](#)] [[PubMed](#)]
35. El Ouardy, K.; Lbouhmadi, R.; Attaoui, H.; Mouzaki, M.; Mouine, H.; Lemkhente, Z.; Mir, Y. Biosynthesis and Characterization of Silver Nanoparticles Produced by *Parachlorella kessleri* and *Cyclotella* spp., and the Evaluation of Their Antibacterial Activity. *Int. J. Mol. Sci.* **2023**, *24*, 10599. [[CrossRef](#)]
36. Abdelmoneim, H.M.; Taha, T.H.; Elnouby, M.S.; AbuShady, H.M. Extracellular biosynthesis, OVAT/statistical optimization, and characterization of silver nanoparticles (AgNPs) using *Leclercia adecarboxylata* THHM and its antimicrobial activity. *Microb. Cell Fact.* **2022**, *21*, 277. [[CrossRef](#)]
37. Gurunathan, S. Rapid biological synthesis of silver nanoparticles and their enhanced antibacterial effects against *Escherichia fergusonii* and *Streptococcus mutans*. *Arab. J. Chem.* **2014**, *12*, 168–180. [[CrossRef](#)]
38. Christopher, J.G.; Saswati, B.; Ezilrani, P. Optimization of Parameters for Biosynthesis of Silver Nanoparticles Using Leaf Extract of *Aegle marmelos*. *Braz. Arch. Biol. Technol.* **2015**, *58*, 702–710. [[CrossRef](#)]
39. Akhtar, M.S.; Swamy, M.K.; Umar, A.; Al Sahli, A.A. Biosynthesis and Characterization of Silver Nanoparticles from Methanol Leaf Extract of *Cassia didymobotyra* and Assessment of Their Antioxidant and Antibacterial Activities. *J. Nanosci. Nanotechnol.* **2015**, *15*, 9818–9823. [[CrossRef](#)]
40. Auten, R.; Davis, J. Oxygen Toxicity and Reactive Oxygen Species: The Devil Is in the Details. *Pediatr. Res.* **2009**, *66*, 121–127. [[CrossRef](#)]
41. Waktole, G. Toxicity and Molecular Mechanisms of Actions of Silver Nanoparticles. *J. Biomater. Nanobiotechnol.* **2023**, *14*, 53–70. [[CrossRef](#)]

**Disclaimer/Publisher's Note:** The statements, opinions and data contained in all publications are solely those of the individual author(s) and contributor(s) and not of MDPI and/or the editor(s). MDPI and/or the editor(s) disclaim responsibility for any injury to people or property resulting from any ideas, methods, instructions or products referred to in the content.